Fluidic Ratchet Based on Marangoni−Bénard Convection

Abraham D. Stroock,† Rustem F. Ismagilov,† Howard A. Stone,‡ and George M. Whitesides*,†

Department of Chemistry and Chemical Biology, and Department of Engineering and Applied Sciences, Harvard University, Cambridge, Massachusetts 02138

Received August 12, 2002. In Final Form: February 24, 2003

A mean flow is observed experimentally in a layer of fluid undergoing Marangoni−Bénard convection over a heated substrate that presents a pattern of asymmetrical grooves. The direction of the mean flow is a function of the temperature difference across the layer and of the thickness of the layer; the direction can be controlled by changing these parameters. This system acts as a fluidic ratchet: the local structure of the thermally driven convection interacts with the asymmetry of the local topographical pattern and causes a net, global flow in the fluid. This fluidic ratchet may be useful in handling fluids on macroscopic and microscopic scales.

Introduction

In the classical demonstration of Marangoni−Bénard (M−B) convection, surface tension drives cellular flows in a uniform layer of fluid that is heated from one side at a flat, solid surface and cooled from the other at an interface with another fluid.[1] The dimensions and forms of the cellular structures that make up the flow are determined by the coupled dynamics of heat transfer and fluid motion and by the thickness of the layer.[2] These types of dynamic structures in uniform systems that are far from equilibrium [M−B convection,[3] Rayleigh−Bénard (R−B) convection,[4] electrohydrodynamic convection,[5,6] Faraday crispations,[7] and others[8]] have been the focus of many studies. We wish to create new fluidic behavior by working with nonuniform systems in which the dynamic structure of the convection interacts with externally imposed patterns.

We[9] and others[10−12] have shown that structures in convecting fluids can be controlled by patterning the imposed temperature gradient or electric field (in the case of electrohydrodynamic convection) across the layer (Figure 1a). In our work with M−B convection, we pattern topographical features on the solid, hot boundary.[9] The work presented here shows that if the topography is in the form of regular, *asymmetric* grooves—grooves with a right−left asymmetry within each period—in the heated substrate of a M−B system (Figure 1a), there is a net secondary flow in the plane of the layer of convecting fluid, in addition to the primary, recirculating flow. This net flow depends on the orientation of the grooves, the difference of temperature across the layer, and the depth of the fluid.[13] This net flow represents a ratcheting effect: a portion of the primary, recirculating component of the convection is transformed into a global flow in the transverse direction. The speed of the transverse flow is small ($\sim 10^{-3}$ cm/s) relative to that of the recirculating component ($\sim$0.1 cm/s). Nonetheless, we believe that this mechanism for creating flow in a direction normal to an applied temperature gradient could be useful for transporting fluids in situations in which temperature gradients are present (e.g., heat transfer applications).

Transverse flows have been predicted and observed experimentally by Hartung et al.[14] and studied numerically by Kelly and Pal[15] and Schmitz and Zimmerman[16] in R−B convection (gravity-driven thermal convection) between hot and cold plates that present sinusoidal topography. In these studies, the asymmetry was induced

* Corresponding author. E-mail: gwhitesides@gmwgroup.harvard.edu.

† Department of Chemistry and Chemical Biology.

‡ Department of Engineering and Applied Sciences.

(1) Koschmieder, E. *Benard Cells and Taylor Vortices*; Cambridge University Press: Cambridge, U.K., 1993.

(2) Manneville, P. *Dissipative Structures and Weak Turbulence*; Academic Press: Boston, 1990.

(3) Loulergue, J. C.; Manneville, P.; Pomeau, Y. *J. Phys. D: Appl. Phys.* **1981**, *14*, 1967.

(4) Ahlers, G. *Phys. Rev. Lett.* **1974**, *33*, 1185.

(5) Manneville, P. *Mol. Cryst. Liq. Cryst.* **1981**, *70*, 1501.

(6) Zimmermann, W.; Kramer, L. *Phys. Rev. Lett.* **1985**, *55*, 402.

(7) Kudrolli, A.; Gollub, J. P. *Physica D* **1996**, *97*, 133.

(8) Cross, M. C.; Hohenberg, P. C. *Rev. Mod. Phys.* **1993**, *65*, 851.

(9) Ismagilov, R. F.; Rosmarin, D.; Gracias, D.; Stroock, A. D.; Whitesides, G. M. *Appl. Phys. Lett.* **2001**, *79*, 439.

(10) Croquette, V.; Schosseler, F. *J. Phys. (Paris)* **1982**, *43*, 1182.

(11) Lowe, M.; Gollub, J. P.; Lubensky, T. C. *Phys. Rev. Lett.* **1983**, *51*, 786.

(12) Zimmermann, W.; Ogawa, A.; Kai, S.; Kawasaki, K.; Kawakatsu, T. *Europhys. Lett.* **1993**, *24*, 217.

(13) Throughout this article, we will refer to the local recirculation (i.e., convection rolls and cells) as the primary flow, and the net flow (i.e., any flow that carries fluid between cells) as a secondary flow.

(14) Hartung, G.; Busse, F.; Rehberg, I. *Phys. Rev. Lett.* **1991**, *66*, 2742.

(15) Kelly, R.; Pal, D. *J. Fluid Mech.* **1978**, *86*, 433.

(16) Schmitz, R.; Zimmermann, W. *Phys. Rev. E* **1996**, *53*, 5993.

(17) Lide, D., Ed. *Handbook of Chemistry and Physics*, 3rd Web ed.; CRC Press: Boca Raton, FL, 2001.

(18) Bird, R.; Stewart, W.; Lightfoot, E. *Transport Phenomena*, 2nd ed.; John Wiley & Sons: New York, 2002.

(19) The typical velocity in M−B convection is $u_M = B\Delta T_s/\eta$, where B (erg/(cm^2 °C)) is the rate of change of the surface tension of the fluid with respect to temperature, η (g/(cm s)) is the viscosity of the fluid, and $\Delta T_s = T_0 - T_s$ is the difference between the average temperatures on the top surface (T_s) and the bottom surface (T_0) of the layer. The typical velocity in Rayleigh−Bénard convection is $u_R = (\rho\alpha g(\Delta T_s)h^2)/\eta$, where ρ (g/cm^3) is the density of the fluid, α (1/ °C) is the thermal expansion coefficient, of the fluid, and h (cm) is the thickness of the layer. $u_R/u_M = (\alpha g\rho h^2)/B$. With $g = 10^3$ cm/s^2 and, for common liquids, $\rho \sim 1$ g/cm^3, $\alpha \sim 10^{-3}$ 1/°C, and $B \sim 10^{-1}$ erg/(cm^2 °C), we find that $u_R/u_M < 1$ for $h < 0.3$ cm.[2,17]

(20) Note that, throughout this article, we report $\Delta T = (T_0 - T_\infty)$, where T_∞ is the air temperature of the room, far from the hot plate. This value of ΔT is proportional to $\Delta T_s = T_0 - T_s$ for a given fluid and thickness of the convecting layer: $\Delta T = ((1 - Bi)/Bi)\Delta T_s$, where $Bi = Hh/k$ is the Biot number, H (erg/cm^2) is the heat transfer coefficient of air, k is the thermal conductivity of the oil, and h is the thickness of the layer of fluid. For silicon oil, $k = 1.5 \times 10^4$ (erg/(s cm °C)). For free convection in air, $H \sim 10^4$ (erg/(s cm^2 °C)). $Bi \sim 0.6h$, with h expressed in centimeters.[18]

10.1021/la026400c CCC: $25.00
Published on Web 04/08/2003

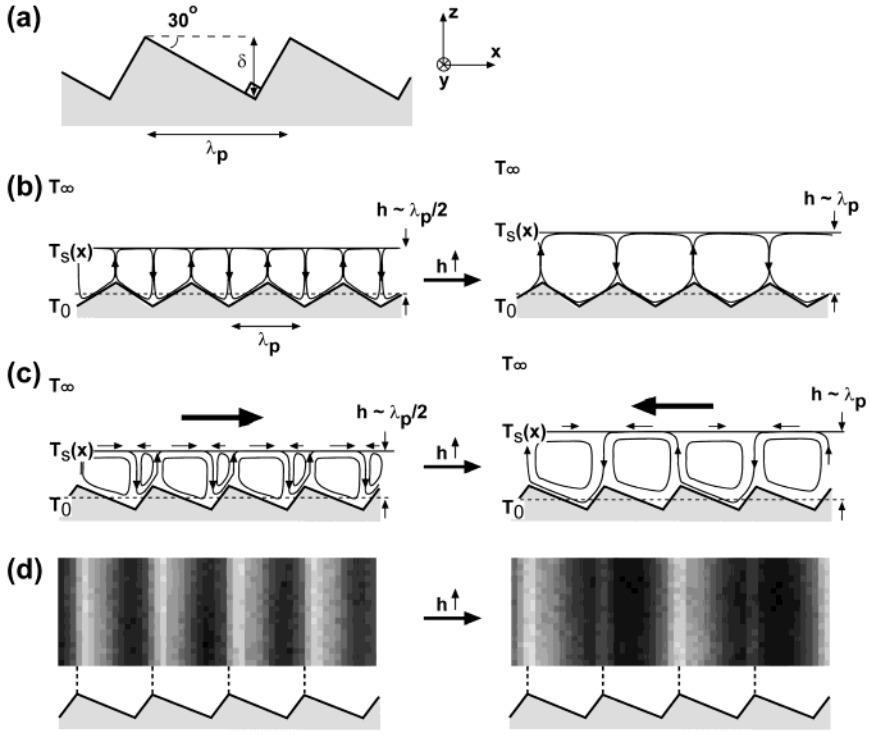

Figure 1. Experimental geometries (a−c) and infrared images of a convecting layer of oil (d). **(**a**)** Schematic diagram showing the cross-sectional form of the grooves; the form is a 30°−60°−90° triangle. The grooves extend into the page, along the *y*-axis. The period of the pattern is λ_p. **(**b**)** Schematic diagrams of period-matched convection over symmetrical grooves. From the left diagram to the right diagram, the average thickness of the layer of fluid, h, passes from $h \sim \lambda_p/2$ to $h \sim \lambda_p$. As h grows, the convection pattern changes from a state in which it has the same period as the grooves (period-matched, on the left) to a state in which it has twice the period of the grooves (period-doubled, on the right). There is no net component of the convection over symmetrical features. **(**c**)** Schematic diagram showing a hypothetical form of the total convection (primary, recirculating flow plus secondary, net flow) over asymmetrical grooves. From the left diagram to the right diagram, the average thickness of the layer of fluid, h, passes from $h \sim \lambda_p/2$ to $h \sim \lambda_p$. As h grows, the convection pattern changes from a period-matched state (left) to a period-doubled state (right). The direction of the net flow (large arrow above layer of oil) for the period-matched case corresponds to the direction observed experimentally at large applied temperature gradients; the direction shown for the period-doubled case is that observed experimentally at all applied temperature gradients (see Results and Discussion). In parts b and c, the temperature of the bottom plate, T_0, the temperature at the interface, $T_s(x)$, and the ambient temperature of the air, T_∞, are shown. Note that in reality the surface of the convecting layer is slightly undulated.[2] (d) Infrared (IR) spectra of a layer of oil over a heated surface patterned with asymmetrical grooves as in parts a and c; $\lambda_p = 0.3$ cm, $\delta = 0.13$, and $h \sim 0.15$ cm on the left, and $h \sim 0.3$ cm on the right. The images show the emission of IR from the layer of oil; the lighter regions indicate qualitatively the position of the warm regions (up-wellings) on the tops of the layer of oil, and the darker regions correspond to the cooler regions (down-wellings). The periodic modulation of the temperature is due to the convection rolls. The convection is period-matched on the left and period-doubled on the right. The position and orientation of the grooves in the aluminum surface are shown schematically below the images. The images were adjusted in Photoshop to increase contrast.

by a phase shift between topography in the top and the bottom solid boundaries; this strategy requires that both the top and bottom surfaces be patterned. The direction of the mean flow depended on the relative phase of the two patterns but not on the magnitude of the applied difference of temperature. We also note that, for applications on the millimeter scale with common liquids (e.g. water, ethanol, silicon oil), R−B convection will be weak; M−B convection is typically the dominant form of convection in layers of liquid that are less than a few millimeters thick.[2,17−20]

Experimental Section

Materials. A cylindrical dish with a depth of 2 cm and an inner diameter of 8.8 cm was machined into a block of copper. A circular aluminum plate (0.5 cm thick and 8.6 cm in diameter) was cut to have a rectangular opening (6.4 cm long and 3.9 wide) through the center. Rectangular aluminum plates to be placed in this opening (0.5 cm thick, 6.3 cm long, and 3.8 cm wide) were machined to have grooves on one side. The circular plate was placed in the center of the floor of the copper dish (0.1 cm of clearance on each side), and one of the grooved plates was placed in the rectangular opening in the circular plate with the grooves facing up. With this assembly in place, the aluminum surface at the bottom of the dish was smooth except in the rectangular region defined by the grooved plate and the narrow gaps at the edges of the aluminum plates. Asymmetric grooves were cut in the form of 30°−60°−90° triangles (Figure 1a). Symmetric grooves were cut in the form of 45°−45°−90° triangles. Silicone oil (Avocado brand, Research Chemicals Ltd., Lancashire, England; $\rho = 0.9$ g cm^{-3} and dynamic viscosity of 0.80 (g/(cm s)) at room temperature) was used for all experiments. For infrared imaging, the grooved plate was coated with a black anodization in order to limit its reflectivity. Dye (Oil Blue, American Cyanamide Co., Brook Bound, NJ) was dissolved in the silicon oil to act as a tracer of the flow.

Methods. For the convection experiments, the copper dish with the assembly of aluminum plates was placed on a temperature-controlled hot plate. The floor of the dish was leveled by eye with a bubble level by adjusting the supports of the hot plate. Oil was added to the dish until the aluminum plates were submerged. The quantity of oil added to the dish was measured by weight. The volume of the oil at different operating temperatures was calculated from the measured weight by using the known density at room temperature and the coefficient of thermal expansion $\alpha = 9.6 \times 10^{-4}$ cm^3/(cm^3 K) (Gelest catalog, Gelest Inc., Tullytown, PA). The depth of the oil above the aluminum plates was calculated from the volume of added oil and the dimensions of the dish and the aluminum plates. Infrared (IR)

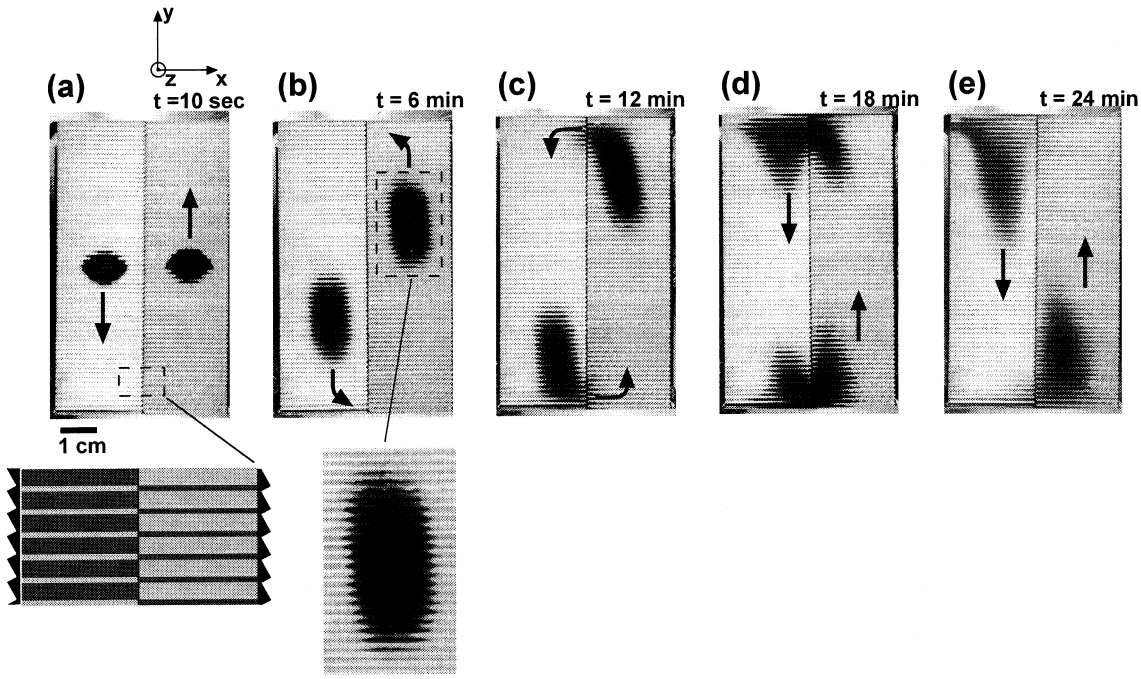

Figure 2. Net secondary flow in a convecting layer of oil over a pattern of asymmetrical grooves. Two drops (~0.02 mL) of dye solution in oil were added to the layer to trace the net flow. **(**a**)** Image of the convecting system 10 s after the drops of dye were added to the layer of oil. **(**b−e**)** Images that show the evolution of the position and shape of dyed regions of oil. The elapsed time after the addition of the dye is indicated above each frame. The pattern of grooves on the bottom plate is shown schematically in the diagram below the image in part a: The pattern was split into a right and a left half; the orientation of the grooves switched abruptly between the right and the left halves of the pattern. The orientation of the grooves in each half is indicated by the orientation of the triangles along the side of the diagram. Below the image in part b, a dyed region is shown in a higher resolution image. The depth of the oil was $h = 0.05$ cm. The dimensions of the grooves were $\lambda_p = 0.1$ cm and $\delta = 0.043$. The black arrows indicate the direction of flow.

images of the convecting layer were taken with an IR camera (model PM-290, FLIR Systems). The top surface of the oil layer was exposed to the atmosphere. The net flow of oil was visualized by adding a drop (0.02 mL) of solution of dye in oil to the convecting layer;[21] the dye solution was heated to the temperature of the hot plate prior to addition. The movement of the dyed region of fluid was used to track the motion of the fluid.

Results and Discussion

Review of Marangoni−Bénard Convection. In Marangoni−Bénard convection, fluid motion is driven from the liquid−air interface. Spatial variations in the temperature of this interface lead to gradients in the surface tension; these gradients drive motion in the underlying fluid. The flow in the fluid is in the form of convection cells or rolls, with fluid descending (down-welling) beneath the cold regions in the surface and rising (up-welling) beneath the hot regions. The up-wellings carry hot fluid from the heated surface to the hot regions of the surface, so that the convection acts as positive feedback to the temperature distribution on the surface. In a layer over a flat surface at a uniform temperature, the variations in the temperature of the top surface (which drive convection) arise spontaneously. This transition occurs when the imposed temperature difference becomes greater than a critical magnitude, ΔT_c.[2] Below this transition, there is no convection; above this transition, a hexagonal pattern of convection cells forms. The width of the cells is approximately equal to twice the thickness, h, of the layer; we call this width the intrinsic period, λ_i, of the M−B convection: $\lambda_i \sim 2h$. The Marangoni number is a dimensionless parameter that measures the tendency of the layer of fluid to convect: $M = hB\Delta T/(\kappa\eta)$, where B (erg/(cm^2 °C)) is the rate of change of the surface tension of the fluid with respect to temperature, η (g/(cm s)) is the viscosity of the fluid, and κ (cm/s^2) is the thermal diffusivity of the fluid. Convection occurs for $M > M_c$, where $M_c = hB\Delta T_c/(\kappa\eta)$ is the critical Marangoni number. It is found experimentally that $M_c \sim 80$.[2] Over a flat bottom boundary, there are no net secondary flows.

Patterned M−B Convection over Asymmetrical Topography. We now describe the effect of the topography of the heated boundary on the primary, recirculating component of the convection. We have previously reported[9] that the addition of periodic, symmetrical topographical features—square, triangular, and hexagonal arrays of posts, and arrays of raised lines—in the heated metal plate below the layer of fluid leads to three changes relative to M−B convection over a flat plate: (1) There is no distinct transition from a pure conduction regime to a convective regime. Instead, the fluid convects for all values of the Marangoni number (i.e., for all $\Delta T > 0$), and there is a jump in the speed of convection as ΔT passes through ΔT_c.[15,22,23] (2) The convection forms patterns that are commensurate—aligned—with the pattern of the topography when the intrinsic period of the M−B convection is near one of the periodicities of the imposed pattern

(21) The addition of dye to the silicone oil is likely to change the surface tension of the oil relative to that of pure oil. We have not attempted to measure this change. The spatial variations in surface tension caused by the addition of the drop of dyed oil should not induce a net Marangoni flow such as the flows that are reported in this article.

(22) The existence of subcritical convection and the jump in speed near $M = M_c$ were predicted by Kelly and Pal for R−B convection.[15] We assess the speed of the convection qualitatively by watching the motion of copper powder in the flow.

(23) In our experiments with topography on the bottom boundary, we take ΔT_c to be the critical temperature difference for the uniform system with a layer of oil of the same thickness. We measure this experimentally.

(e.g., $\lambda_i \sim \lambda_p$ or $2\lambda_p$, where λ_p is the principal periodicity of the imposed topography—Figure 1b). (3) The pattern of convection switches abruptly between different commensurate structures as λ_i varies (Figure 1b). The case of convection over symmetrical grooves is shown schematically in Figure 1b: one period of the convection pattern fits over one period of the topography (period-matched) or over two periods of the topography (period-doubled). Over asymmetrical features, the primary convection also occurs for all values of M and in patterns that are period-matched or period-doubled with respect to the topographical patterns (Figure 1c and d). As suggested in the schematic diagrams in Figure 1c and shown in the infrared (IR) images in Figure 1d, the convection rolls over asymmetrical features are themselves asymmetrical; the downwellings are not positioned midway between the upwellings.

Net Flow in M−B Convection over Asymmetrical Grooves. M−B convection has a net secondary flow when the layer of oil is heated over a surface with asymmetrical grooves. We note that this secondary flow occurs in addition to the primary recirculating flow that was discussed in the previous section. No such net flow was observed either over flat surfaces or over symmetrical topographical features. The photographs in Figure 2 show the evolution of two drops of dye added to a layer of oil ($h = 0.05$ cm) undergoing period-matched convection above the critical Marangoni number ($\Delta T = 120$ °C; $\Delta T_c = 107$ °C). The bottom plate presents a pattern of asymmetrical grooves ($\lambda_p = 0.1$ cm, $\delta = 0.043$ cm) with opposite orientations on the right and left halves of the plate: on the left half of the plate, the steeply sloping sides of the grooves face the top of the page; on the right side of the plate, the steeply sloping sides face the bottom of the page (see diagram in Figure 2a). The displacement of the spots of dye in Figure 2 demonstrates that there was a net flow in the plane of the layer of fluid. The fact that the spots of dye moved in opposite directions over oppositely oriented grooves indicates that the direction of net flow depends on the orientation of the asymmetry of the grooves. The average speed of the net secondary flow was $\sim 3 \times 10^{-3}$ cm/s in the plane of the film.

The dyed region broadened more rapidly along the direction of the net motion (along y) than perpendicular to that motion (along x). We attribute this anisotropic broadening to convective dispersion through convection rolls (the primary flow) that were oriented along the grooves, for the value of ΔT used in the experiments shown in Figure 2.[24] In experiments in which the convection was in the form of cells (i.e., for larger ΔT and thicker layers), the broadening along both x and y was comparable; in these cases the recirculation was along both x and y.

We extracted average flow velocities from images such as those shown in Figure 2 by measuring the distance between the centers (estimated by eye) of the spots of dye in a sequence of images. Figure 3 shows two sets of velocity data for layers with fixed average thickness ($h \sim \lambda_p/2$ and $h \sim \lambda_p$) as a function of the temperature difference, ΔT: The filled circles (●) represent the velocity for period-matched rolls. In this case, the net flow is negative (the sign is defined in the inset) with increasing magnitude below $\Delta T < 80$ °C; above this temperature difference, the net flow velocity becomes positive and its magnitude grows more rapidly. The flow speed appears to plateau for $\Delta T > 130$ °C. The open diamonds (◇) represent the net velocity for period-doubled cells; this velocity is positive for the temperature range studied. The locations of the critical temperature differences, ΔT_c (determined experimentally), are indicated for both the period-matched ($\Delta T_{c,pm}$) and the period-doubled cases ($\Delta T_{c,pd}$). The speed of convection and the amplitude of the net flow both increase rapidly above the critical Marangoni numbers, as was predicted by Kelley and Pal for Rayleigh−Bénard convection between surfaces with undulating topography.[15]

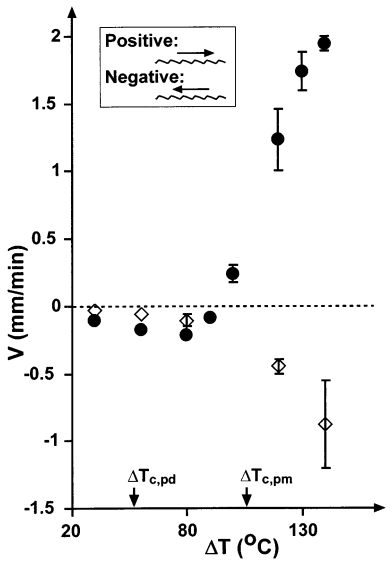

Figure 3. Net flow velocity (cm/min) as a function of temperature difference $\Delta T = (T_\infty - T_0)$ across a layer of oil over asymmetrical grooves ($\lambda_p = 0.1$ cm, $\delta = 0.043$ cm). The flow velocities were measured on images such as those in Figure 2; displacements were measured as the distance between the centers of the distribution of dye in subsequent images. The filled circles (●) represent the velocities for a layer of silicone oil with average thickness $h = 0.05$ cm, for which the convection pattern is *period-matched* with the grooves in the plate; in this case, the flow changes direction at $\Delta T \sim 90$ °C. The open diamonds (◇) represent the velocities for a layer of the same oil with $h = 0.1$ cm, for which the convection is *period-doubled* with respect to the grooves; in this case, no change in the direction of flow was observed. The symbols $\Delta T_{c,pm}$ and $\Delta T_{c,pd}$ indicate the approximate positions of the critical Marangoni temperature for unperturbed layers of oil (i.e., heated over flat substrates) with thicknesses that correspond to *period-matched* and *period-doubled* cases. Error bars represent the largest deviation from the average velocity found within a single experiment. The variability of the errors is principally due to variations in the size of the drop of dyed oil used as a tracer; larger drops lead to less precise measurements of position. The error bars are shown only when they are larger than the symbol. The sign of the net flow is defined in the inset.

Conclusions

A net flow can be generated in a thin film of liquid with the addition of a simple topographical pattern to the heated lower boundary below. The use of asymmetrical topographical features allows this net flow to form in the presence of a single patterned surface; this approach is simpler than previously proposed methods that require topography on two surfaces[14] or patterned heating superimposed on topography.[15,16] Our system, based on M−B convection, is appropriate for millimeter-scale applications such as integrated fluid handling for chemical processes. In particular, the net flow could act as a pump driven by

(24) The recirculation of the fluid assists molecular diffusion along the direction orthogonal to the axis of rolls (along y): When dye diffuses into a convection roll, the recirculating flow carries the dye rapidly (compared to diffusion) across the width of the roll. Some of the dye can then reach the next roll by diffusing a short distance (compared to the width of the roll) along y.

the excess heat from another process in the device (e.g. heaters for polymerase chain reactions[25]).

The direction of the mean flow in this system changes with variations in the magnitude of the temperature difference across the layer of oil and in the thickness of the layer of oil. This behavior is unexpected, because the direction of flows driven with steady pressure gradients and electric fields does not change with the magnitude of the applied fields or with the size of the system. In the case studied here, the sensitivity of the net flow to these parameters is due to the dependence of the flow on the complicated, nonlinear dynamics of the thermal convection.

(25) Kopp, M. U.; Mello, A. J. d.; Manz, A. *Science* **1998**, *280*, 1046.

Acknowledgment. The work in the laboratory of G.M.W. was supported by the Department of Energy (DE-FG02-OOER45852). The work of both G.M.W. and H.A.S. was supported by NSF MRSEC DMR-9809363 and DARPA.

LA026400C